

Multi-Stage Monte Carlo Tree Search for Non-Monotone Object Rearrangement Planning in Narrow Confined Environments

Hanwen Ren and Ahmed H. Qureshi

Abstract—Non-monotone object rearrangement planning in confined spaces such as cabinets and shelves is a widely occurring but challenging problem in robotics. Both the robot motion and the available regions for object relocation are highly constrained because of the limited space. This work proposes a Multi-Stage Monte Carlo Tree Search (MS-MCTS) method to solve non-monotone object rearrangement planning problems in confined spaces. Our approach decouples the complex problem into simpler subproblems using an object stage topology. A subgoal-focused tree expansion algorithm that jointly considers the high-level planning and the low-level robot motion is designed to reduce the search space and better guide the search process. By fitting the task into the MCTS paradigm, our method produces optimistic solutions by balancing exploration and exploitation. The experiments demonstrate that our method outperforms the existing methods regarding the planning time, the number of steps, and the total move distance. Moreover, we deploy our MS-MCTS to a real-world robot system and verify its performance in different confined environments.

I. INTRODUCTION

Object rearrangement planning in narrow, confined spaces such as cabinets, shelves, and fridges is essential for robots working in such environments. For example, robots must rearrange objects by grouping the same type for maintenance needs and create particular patterns to use the confined space better. Object rearrangement planning is generally known as NP-hard [1] because the planner needs to figure out the moving order of the objects and the intermediate relocation regions. This problem can further be categorized as follows based on the moving count of objects and robot actions. The monotone instances are where each object can be relocated at most once, and the non-monotone instances are where they can be relocated multiple times in the scene. Regarding robot movements, the prehensile instances consider robot pick-and-place actions, whereas non-prehensile instances use push actions. This work focuses on prehensile non-monotone object arrangement planning problems in narrow, confined spaces shown in Figure 1. The confined spaces setting introduces an extra constraint on the robot’s motion compared to tabletop environments. In tabletop environments, robots can grasp objects from the top and use the space above the objects to avoid collisions during relocation. However, in confined environments with a covered top and a side opening, the objects can only be accessed from the side. Hence, robots always occupy a certain amount of space



(a) Start object arrangement



(b) Goal object arrangement

Fig. 1: Object rearrangement achieved by our MS-MCTS method in a narrow confined space. The top is open for depiction purposes while the red cable placed at the front forms the ceiling of the environment.

during the motion, resulting in fewer regions for objects to be placed and a high chance of object-to-object and object-to-robot collisions.

Most existing works solve the rearrangement planning problem using tree search methods [2], [3]. The start arrangement is often defined as the root, and the tree keeps growing until the goal arrangement is achieved. The parent and child tree nodes are linked with a single object movement, i.e., one object is relocated to another region by the robot in a collision-free manner. Once the goal arrangement is found, the algorithm backtracks and recovers the entire plan. For monotone arrangement planning instances with a fixed maximum search depth, the planner’s runtime is $O(n!)$ since it needs to check all the permutations of the object relocation order [4]. However, when it comes to

non-monotone instances, the planner does not have prior knowledge about the search depth, as all objects are subject to be moved at any given step. In addition, without proper guidance on the tree expansion process, the effort can be wasted on redundant object relocation actions that do not help to achieve the goal. Thus, the standard tree search method will not work anymore because of the enormous search space.

In this paper, we solve prehensile non-monotone object rearrangement planning problems in narrow, confined spaces using the proposed Multi-Stage Monte Carlo Tree Search (MS-MCTS) method. Our approach performs well in simulated test cases and outperforms the state-of-the-art baselines by an adequate margin. We also deploy the method to real-world scenarios and verify its real-world generalization ability. In summary, the main contributions of the work are listed as follows:

- An non-monotone object rearrangement planner that finds high-quality solutions by fitting the problem into the MCTS paradigm. Our method suits real-world robotics systems of different configurations.
- A specially designed subgoal-focused tree expansion algorithm that jointly considers the high-level relocation planning and low-level robot motion planning, which constrains the search within a limited sub-space.
- A novel object relocation order heuristic helps the planner decouple the complicated problem into simpler sub-problems, which is proven suitable for the narrow, confined spaces setting.
- A computationally efficient robot motion planner that minimizes the swept volume of the robot actions.

II. RELATED WORK

Object rearrangement planning in various environments is an active and widely researched problem in robotics, which is also a frequently occurring instance in the field of Navigation Among Movable Obstacles (NAMO) [5], [6] and Task And Motion Planning (TAMP) [7], [8]. Since it needs to consider both the high-level task planner and the low-level motion planner in environments with movable objects, the problem is generally considered NP-hard. Existing works solve the rearrangement planning problem under different settings. [9], [10], [11], [12] perform the planning on tabletop environments utilizing tree search with modified growing strategies or search hierarchy followed by backtracking. Others [13], [14], [15], [16] put the recent advancement of the deep neural network into play and let the planning agent learn the underlying logic of various moves using the collected dataset. Aside from the open workspace, [17], [18], [19], [20] assume more constrained environments like the cabinets or other confined spaces with only one opening in the front, which are more common in real-world scenarios. Their strategies include performing intelligent expansions or pre-pruning the search trees so that invalid actions can be filtered out at early stages. These moves shrinks the search space and increases efficiency.

Compared with our method that finds an optimistic solution, most of them only aim to find a valid solution in a depth-first search manner without considering the quality of the resulting plans, which can be defined by criteria such as the total number of steps or the total relocation distance.

In order to find high-quality optimistic solutions, the Monte Carlo Tree Search (MCTS) [21] has recently been applied to the rearrangement planning problems. MCTS has been proven extremely useful in balancing the exploration and exploitation during the search process, resulting in strong performances. The AlphaGo, AlphaZero [22], [23], [24] took advantage of MCTS and beat the top-ranked human go player in 2016. In rearrangement planning problems, [25] use MCTS to achieve both efficiency and scalability in tabletop environments. [26], [27] fit the non-prehensile object rearranging and sorting tasks into the MCTS paradigm to achieve decent performance. Different from these works, we use the MCTS in the confined spaces setting with specially designed algorithms to guide the expansion and simulation process, resulting in decent performances in the runtime and the plan quality.

III. PROBLEM FORMULATION

Let a confined workspace with one narrow opening at the front be denoted as $\mathcal{W} \subset \mathbb{R}^3$. In this confined space, $n \in \mathbb{N}$ identical but uniquely labeled cylindrical objects with radius b reside and are denoted as $\mathcal{O} = \{o_1, \dots, o_n\}$. The ground surface of the workspace has many placement location candidates $p \in \mathcal{P} \subset \mathbb{R}^2$ where the geometric center of the objects' bottom surface can be placed. The placement locations associated with all objects at step t form the object arrangement $a^t = \{p_1^t, \dots, p_n^t\} \subset \mathcal{A}$, where \mathcal{A} is the arrangement space. $a^t[o_i] = p_i^t$ denotes that object o_i locates at region p_i^t in arrangement a^t . A robot arm \mathcal{M} equipped with a gripper is placed in front of the workspace opening at location p_m to perform prehensile object relocation actions. One relocation action r^t at step t involves robot actions listed as reaching, picking, placing, and retrieving. While performing such actions, the robot follows a certain manipulation path $\pi(r^t) = \{q_0^t, \dots, q_k^t\}$, where $q_i \in \mathcal{Q}$. The $\mathcal{Q} \subset \mathbb{R}^d$ is a d -dimensional arm configuration space. The volume occupied by the robot arm during a relocation action is represented as $V(\pi(r^t))$. A relocation action involving object o_k at step t is valid if it satisfies the collision constraint, written as $V(\pi(r^t)) \cap V(a^t \setminus a^t[o_k]) = \emptyset$, where the term, $V(a^t \setminus a^t[o_k])$, is the space occupied by all other objects except the one that is currently being relocated.

Using the notations above, the non-monotone object rearrangement planning problem is formally defined as follows. Given n -objects start arrangement a^s and goal arrangement a^g , find a sequence of valid and optimistic robot actions $R = \{r^0, r^1, \dots\}$ that relocates all objects from their start regions to the goal regions.

IV. METHODOLOGY

This section formally introduces the proposed Multi-Stage Monte-Carlo Tree Search (MS-MCTS) object rearrangement

task planner and the related modules in detail.

A. Linear Motion Planner

We design a linear motion planner to move the gripper to the objects and perform prehensile actions. In the confined spaces setting, where the robot cannot use the space on the Z axis to avoid collisions, the planner first aims the gripper toward the objects and then moves it linearly in the XY plane while maintaining a fixed height on the Z axis. The robot configurations for linear movement $\pi(r^t)$ can be obtained by calculating the Inverse Kinematics (IK) [28] on the discretized points along the path. To relocate an object o_i from its current region p_i^t to the next region p_i^{t+1} , the gripper first moves from its home location p_m to p_i^t , picks the object up, and retrieve it back. Then it goes to p_i^{t+1} , places the object, and returns to p_m . In order to check collisions, the robot's swept volume $V(\pi(r^t))$ during the linear movement is constructed by a rectangular tunnel with length h_q , width w_q , tilted at angle θ_q shown in Figure 2. In the rest of the paper, we use the terms picking tunnel and placing tunnel to denote the swept volume of the robot's prehensile actions. The tunnel parameters h_q and θ_q that moves the gripper from p_m to an object with radius b located at p_i^t can be calculated as:

$$h_q = \|p_i^t - p_m\|_2 + b \quad (1)$$

$$\theta_q = \arccos\left(\frac{\mathbf{i} \cdot (p_i^t - p_m)}{\|p_i^t - p_m\|_2}\right) \quad (2)$$

where \mathbf{i} is the unit vector on the positive X axis. The parameter w_q is the robot's maximum width when the gripper moves linearly. There are three advantages of our linear motion planner. First, it is a general method that suits all robots of various configurations. Second, the collision between the objects and the robot motion tunnel can be efficiently checked by the Separating Axis Theorem [29]. The prehensile actions are valid when the associated tunnels are collision-free. Third, the linear motion planner minimizes the swept volume, resulting in a higher probability of finding valid solutions.

B. Object Stage Topology Generation

We generate an object stage topology that orders the objects' placements based on the goal regions' longitudinal distances from robot p_m . It prioritizes objects that are to be placed farther behind than closer to the robot. Recall the linear motion planner introduced above. The objects placed at their goal regions in the front of the environment are more likely to block the objects with goal regions further back, which means they must be relocated to a buffer region elsewhere before returning, wasting the steps of getting them to the goal regions in the first place. Thus, it is more appropriate to relocate objects in the decreasing order of their longitudinal distances between their goals and the robot. After sorting, we still represent the object list as $\mathcal{O} = \{o_1, \dots, o_n\}$, where the subscripts now denote the generated order.

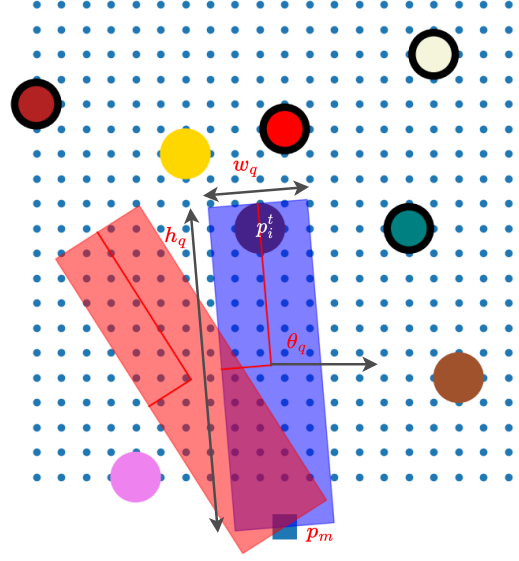


Fig. 2: The gripper at p_m uses the collision-free picking tunnel (blue) and placing tunnel (red) generated from our linear motion planner to relocate the object at p_i^t . Objects with a black contour are already placed at their goal regions.

C. Single-Stage MCTS planner

Our Single-Stage MCTS (SS-MCTS) planner aims to move one specific object o_k from its current region $a^t[o_k]$ to the goal $a^g[o_k]$. In other words, the search halts when the objective $a^t[o_k] = a^g[o_k]$ is achieved at some step $t' \geq t$. To better present our ideas, we introduce several new notations as follows. Assume we are now in the SS-MCTS planner that focuses on the k -th object o_k in the generated topology, and the current step count is t . All the objects that have been relocated to their goal regions form a set of static objects $\mathcal{O}_s = \{o_1, \dots, o_{k-1}\}$ and the rest are represented as $\mathcal{O}_r = \{o_k, \dots, o_n\}$. In the SS-MCTS focusing on object o_k , only the objects in \mathcal{O}_r are subject to be relocated. The current arrangement a^t and the goal arrangement a^g contain the most up-to-date pairwise corresponded elements denoting objects' current/goal regions. The following paragraphs reveal the details of our SS-MCTS by fitting them into the standard MCTS paradigm.

Selection: The SS-MCTS planner balances the exploration and exploitation by utilizing the Upper Confidence Bound (UCB) [21]:

$$U(c) = \frac{w(c)}{n(c)} + 2\sqrt{\frac{\log(n(p))}{n(c)}} \quad (3)$$

where p and c are the parent and the child tree nodes, the $w()$ function represents the cumulative reward while the $n()$ function records the number of times a specific tree node has been visited so far. The parent and child tree nodes are linked by robot action r^t that relocates a single object o_i in \mathcal{O}_r from region p_i^t to p_i^{t+1} , forming a new arrangement a^{t+1} . The associated reward function value is assigned as the negation of the Euclidean distance between two regions, i.e., $-\|p_k^t - p_k^{t+1}\|_2$. In the selection process, starting from

the root of the SS-MCTS, we select a leaf node with current arrangement represented as a^{t+b} , where b is the number of robot motion performed starting from a^t , by going through successive child nodes maximizing the UCB values. If the selected leaf node has already been visited, the expansion algorithm introduced below will be applied to it and grow the tree further.

Algorithm 1: get_blocking_objects

Data: o_k, a^t, a^g, O_r
// object of interest, current arrangement, goal arrangement and remaining objects
Result: O_b *// objects that block the objective*

```

1  $O_b = \emptyset$ 
2  $V(\pi(r_{picking})) = \text{LMP}(a^t[o_k])$ 
3  $V(\pi(r_{placing})) = \text{LMP}(a^g[o_k])$ 
4 for  $o_i \in O_r \setminus o_k$  do
5    $flag\_p = \text{collision}(a^t[o_i], V(\pi(r_{picking})))$ 
6    $flag\_d = \text{collision}(a^t[o_i], V(\pi(r_{placing})))$ 
7    $V(\pi(r_{picking}^i)) = \text{LMP}(a^t[o_i])$ 
8    $flag\_i = \text{collision}(a^g[o_k], V(\pi(r_{picking}^i)))$ 
9   if  $flag\_p$  or  $flag\_d$  or  $flag\_i$  then
10      $O_b.add(o_i)$ 
11 return  $O_b$ 

```

Algorithm 2: new_region

Data: o_i, o_k, o_d, a^t, a^g
// object to remove, object of interest, the dependent object, current arrangement and goal arrangement
Result: $P_i^r = \{p_i^1, \dots, p_i^m\}$ *// new regions*

```

1  $P_i^r = \emptyset$ 
2  $V(\pi(r_{picking})) = \text{LMP}(a^t[o_k])$ 
3  $V(\pi(r_{placing})) = \text{LMP}(a^g[o_k])$ 
4  $V(\pi(r_{picking}^d)) = \text{LMP}(a^t[o_d])$ 
5 for region candidates  $p_i \in P$  do
6   if  $\text{collision\_free}(p_i, \{a^t \setminus a^t[o_i], V(\pi(r_{picking}^d)), V(\pi(r_{picking})), V(\pi(r_{placing})))\})$ 
7     then
8        $V(\pi(r_{placing}^i)) = \text{LMP}(p_i)$ 
9       if  $\text{collision\_free}(V(\pi(r_{placing}^i)), a^t \setminus a^t[o_i])$ 
10         then
11            $P_i^r.add(p_i)$ 
12           if  $\text{size}(P_i^r) = m$  then
13             break
13 return  $P_i^r$ 

```

Expansion: We present an efficient subgoal-focused expansion algorithm that reduces the search space, which in result leads to better runtime performance. The objective of the SS-MCTS is carried over to be the subgoal, i.e., relocating object o_k to its goal region, and the tree grows focusing

Algorithm 3: Expansion

Data: $\text{TreeNode } T_p(o_k, a^t, a^g, O_r)$
Result: $\text{TreeNode } T_c(o_k, a^{t+1}, a^g, O_r)$

```

1  $O_b = \text{get\_blocking\_objects}(o_k, a^t, a^g, O_r)$ 
2 if  $O_b \neq \emptyset$  then
3   while True do
4      $O'_b = \emptyset$ 
5     for  $o_i \in O_b$  do
6        $V(\pi(r_{picking}^i)) = \text{LMP}(a^t[o_i])$ 
7        $O_b^{ip} = \text{collision\_objs}(O_r \setminus o_i, V(\pi(r_{picking}^i)))$ 
8       if  $O_b^{ip} = \emptyset$  then
9          $V(\pi(r_{placing}^i)) = \text{LMP}(a^g[o_i])$ 
10         $O_b^{id} = \text{col\_objs}(O_r \setminus o_i, V(\pi(r_{placing}^i)))$ 
11        if  $O_b^{id} = \emptyset$  and  $\text{Valid}(a^g[o_i], o_k)$  then
12           $T_p.add\_child(T_c(a^{t+1}[o_i] = a^g[o_i]))$ 
13        else
14           $P_i^r = \text{new\_region}(o_i, o_k, \text{none}, a^t, a^g)$ 
15          for  $p_i^r \in P_i^r$  do
16             $T_p.add\_child(T_c(a^{t+1}[o_i] = p_i^r))$ 
17        else
18          for  $o_j \in O_b^{ip}$  do
19             $V(\pi(r_{picking}^j)) = \text{LMP}(a^t[o_j])$ 
20            if  $\text{collision\_free}(O_r \setminus o_j, V(\pi(r_{picking}^j)))$ 
21              then
22                 $P_j^r = \text{new\_region}(o_j, o_k, o_i, a^t, a^g)$ 
23                for  $p_j^r \in P_j^r$  do
24                   $T_p.add\_child(T_c(a^{t+1}[o_j] = p_j^r))$ 
25                else
26                   $O'_b.add(o_j)$ 
27            if  $T_p.children$  then
28              break
29            else
30               $O_b = O'_b$ 
31          else
32             $T_p.add\_child(T_c(a^{t+1}[o_k] = a^g[o_k]))$ 
33 return  $T_p.child[0]$ 

```

on it. In order to achieve the subgoal, first, the planner finds the objects currently blocking the robot's motion from relocating o_k using Algorithm 1. It starts from calculating the picking tunnel $V(\pi(r_{picking}))$ and the placing tunnel $V(\pi(r_{placing}))$ using our linear motion planner (denoted as the LMP function) based on the current and goal region of o_k (line 2-3). All remaining objects except o_k should be

moved to other regions if they are inside the two tunnels, as mentioned earlier (line 5-6). In addition, because o_k becomes a static object in the following SS-MCTS focusing on o_{k+1} , the planner needs to ensure the remaining objects can still be accessed after placing o_k in its goal region. Thus, objects whose picking tunnel $V(\pi(r_{picking}^i))$ intersects with o_k at its goal region are added to the blocking object list O_b as well (line 7-8).

Next, we propose Algorithm 2 to generate new valid region candidates for the objects $o_i \in O_b$. A helper function called `collision_free()` detects whether there is a collision between the inputs. The valid region candidate p_i for object o_i should not collide with the following elements: 1. all the regions currently occupied by other objects $a^t \setminus a^t[o_i]$. 2. the picking and placing tunnels of o_k . 3. the picking tunnel of the dependency object o_d (line 2-6). The dependency object will be explained later when presenting the complete expansion algorithm. Given the region candidates, the placing tunnels of them should not collide with any existing objects except o_i itself (line 9-10). During the actual execution, we sort the potential region candidates P by the increasing distance to the current one so that it better aligns with the reward function. An upper bound m is set to prevent the tree from growing too wide while still maintaining decent performance.

The complete expansion algorithm is shown in Algorithm 3 with the help of an additional helper functions. The `collision_objs` function (line 7, 10) takes an object list and a tunnel as inputs. It returns all objects in the list that collides with the input tunnel. Also, the notation O_b^{ip} and O_b^{id} denote all objects that blocks the picking and placing tunnels of object o_i , respectively. The algorithm starts at parent tree node T_p by checking if both the picking and placing tunnels for o_k are collision-free, if so, only one child tree node T_c that puts o_k directly to its goal region is created, which means the subgoal is achieved (line 1, 2, 31). Otherwise, the blocking objects $o_i \in O_b$ are further divided into the following three categories where different strategies are applied: 1. For o_i that has both picking and goal-region placing tunnels collision-free along with the fact that placing o_i at its goal region does not block the tunnels for o_k (checked by the `Valid()` function), it will be directly relocated to the goal region $a^g[o_i]$ (line 12). 2. If only the picking tunnel for o_i is available, valid regions are proposed using Algorithm 2 and added to the tree (line 14-16). 3. If even the picking tunnel for o_i is not available, the algorithm first finds all objects O_b^{ip} blocking it. For each object $o_j \in O_b^{ip}$ that can be accessed, new regions are proposed with the dependency object setting as o_i so that the picking tunnel of o_i can be cleared (line 18-23). The search process focusing on the subgoal keeps running until some candidates are found (line 26-29). The expansion algorithm returns the first child node found during the process, from where the simulation starts (line 31). The high-level ideology of our expansion algorithm is that it grows the tree by gradually moving blocking objects out of the picking and placing

tunnels for o_k . Eventually, both tunnels are collision-free, and our subgoal is fulfilled. Furthermore, our method can handle non-monotone problems where o_k must be relocated to a buffer region before other objects because o_j can potentially be set as o_k during the search process (line 18).

Simulation: This part follows the standard MCTS pipeline. During the rollout process, one of the candidates is selected randomly if new regions are proposed by Algorithm 2. The termination condition is satisfied when the object of interest o_k is relocated to its goal region.

Back-propagation: The reward function is set to be the negation of the accumulated region displacement distances when the simulation ends, as it is the term we seek to minimize. All tree nodes from the leaf where the simulation starts until the root receive the reward and one visited count during the backpropagation process.

The SS-MCTS planner halts when the current tree node achieves the objective. The sub-plan $\{r^t, \dots, r^{t+q}\}$ can be recovered by traversing back from the current node to the root.

Algorithm 4: Solution Conversion

Data: $P = (o_{(1)}, o_{(2)}, \dots, o_{(k)})$
 /* solution that does not obey our object stage topology */
Result: $MS - MCTS = (SM_{o_1}, SM_{o_2}, \dots, SM_{o_n})$
 /* MS-MCTS solution that contains P */

```

1  $MS - MCTS = \emptyset$ 
2 for  $o_i \in (o_1, o_2, \dots, o_n)$  do
3    $i = P.\text{find\_last}(o_i)$ 
4   if valid( $i$ ) then
5      $SM_{o_i} = P[0 : i]$ 
6      $P = P[i + 1 : \text{end}]$ 
7   else
8      $SM_{o_{yi}} = \emptyset$  /* dummy tree */
9    $MS - MCTS.\text{add}(SM_{o_i})$ 
10 return  $MS - MCTS$ 

```

D. Multi-Stage MCTS planner

The MS-MCTS planner comprises n ordered SS-MCTS. The SS-MCTS at index i sets its object of interest as o_i from the generated object stage topology introduced above. By extracting and combining all the sub-plans from the SS-MCTS planners, we get the global plan $R = \{r^0, r^1, \dots\}$ that moves all objects from the start arrangement a^s to the goal arrangement a^g . If a valid solution P does not obey the generated object stage topology, we show that it can still be covered using Algorithm 4. Starting from an empty MCTS tree array (line 1), for each object o_i following our object stage topology, we try to find the last occurrence of it in P (line 3). Suppose such appearances can be found, an SS-MCTS (denoted as SM) with o_i setting as the objective is added to the tree array. The SS-MCTS contains a segment of the solution P from the start to the last occurrence of o_i , which means this SS-MCTS rearranges all objects in

Rearrangement Task planner	Easy & Medium cases				
	Success rate (%) \uparrow	Number of steps \downarrow	Planning time (s) \downarrow	Relocation distance \downarrow	Displacement distance \downarrow
BiRRT(mRS)	85	15.83 \pm 7.97	1.32 \pm 2.31	419.32 \pm 221.59	150.59 \pm 72.33
PERTS(CIRS)	81	27.99 \pm 33.74	0.34 \pm 0.95	622.49 \pm 673.21	259.74 \pm 293.48
MS-MCTS (ours)	99	10.31 \pm 3.05	0.38 \pm 0.51	224.90 \pm 74.21	63.21 \pm 19.56

Rearrangement Task planner	Hard cases				
	Success rate (%) \uparrow	Number of steps \downarrow	Planning time (s) \downarrow	Relocation distance \downarrow	Displacement distance \downarrow
BiRRT(mRS)	3	18.67 \pm 6.60	7.19 \pm 0.65	518.40 \pm 205.38	190.66 \pm 85.29
PERTS(CIRS)	40	52.17 \pm 30.06	1.90 \pm 2.48	1071.94 \pm 613.35	440.92 \pm 246.87
MS-MCTS (ours)	77	17.72 \pm 3.02	1.21 \pm 0.88	402.00 \pm 75.24	107.34 \pm 21.47

TABLE I: Experiments results reflect that our MS-MCTS outperforms the baseline methods in all metrics.

this segment to their goal regions. Such conversion makes sense because our SS-MCTS is a single-object-focused non-monotone task planner in which all objects except the static ones are subject to relocation. After the partition, P will be reduced to a plan that does not contain o_i anymore (line 5-6). If the current solution P does not contain o_i , we can add an empty SS-MCTS to the tree array as it has been covered in a former SS-MCTS planner (line 8). When the algorithm returns, we get an planner array MS-MCTS = $(SM_{o_1}, SM_{o_2}, \dots, SM_{o_n})$ containing solution P .

V. EXPERIMENTS

A. MS-MCTS Task Planner

We create randomly generated start and goal arrangements of five increasing difficulty levels to examine the performance of our MS-MCTS. The environment has a dimension of 20 by 20 units with 4-8 objects inside. All objects are presented by circles with a radius 1 unit and they are placed with a minimal distance of 4 units between the centers to leave some grasping space for the gripper. The picking and placing tunnel width is set to be 4 units. The 4 objects cases are considered to be easy, 5-6 to be medium, and 7-8 to be hard. In the eight objects scenario, at any given time step, on average, 36% of the environment space is occupied by robot tunnels and objects (max 57%, min 16%), making these cases hard to solve. For each difficulty level, 80 cases are generated to understand the method's performance comprehensively. Aside from our MS-MCTS, two additional non-monotone planner baselines, BiRRT(mRS) [4] and PERTS(CIRS) [17], are implemented to compare against our method. BiRRT(mRS) follows the BiRRT algorithm with tree nodes denoting different arrangements. The mRS monotone solver connects different tree nodes and finally forms the complete plan. PERTS(CIRS) divides the hard non-monotone case into a sequence of monotone cases. It utilizes perturbations to find valid buffer regions when the tree cannot grow further with the CIRS monotone solver. We use the following metrics for quantitative evaluation:

- **Success rate:** The percentage of successfully solved instances in 80 cases. Cases that are not solved within 10 seconds are considered as failures.
- **Planning time:** The time used in the successful cases before the task planner finds a valid solution.
- **Number of steps:** The number of steps (relocate one object) needed to achieve the goal arrangement.

- **Relocation distance:** The sum of relocation distance of all objects. The relocation distance is the total distance moved inside the picking and placing tunnels.
- **Displacement distance:** The sum of displacement distance of all objects. The displacement distance is the Euclidean distance between the start and end regions.

Table I lists the test results. The last four metrics are presented by taking the average among all successful cases. We separate the difficulty levels to better showcase the strong performance of our method. Detailed visual comparisons of the success rate and the number of steps are shown in Figure 4. Our MS-MCTS not only outperforms the baselines in all metrics but also stays reasonably stable within the same difficulty level, which can be seen from the relatively small standard deviation. In addition, the increasing difficulty levels have less effect on our method than others as the relocation distance grows almost linearly at a low rate. At the same time, the performance of the baselines drops significantly with respect to the increasing difficulty levels. In the most challenging settings, our MS-MCTS has a success rate that is three times as high as the best baseline PERTS(CIRS) while still maintaining an average step count that is 29% of it. Due to the multi-stage setting, adding more objects means growing more SS-MCTS, which gives our method better scalability.

B. Real Robot Experiments

1) *Object Rearrangement Planning:* We deploy our MS-MCTS task planner on an UR5e robot arm manipulator equipped with a Robotiq 2F-85 gripper. Since UR5e has a pre-built workspace linear motion planner, we use it to pick and place objects. For robots without this functionality, the linear planner can also be achieved by pre-computing the IK on evenly spaced points along the path offline. Using the linear planner, the total time consumption for the rearrangement planning tasks is just the algorithm runtime plus the robot motion time. Our objects are cylindrical tubes with colored coating indicating their ids. For each experiment, the goal arrangements a^g always have clear and structured patterns, while the start arrangements a^s are randomly generated. The program takes a^s, a^g as inputs, figures out the plan, and executes using the real robot manipulator.

The first set of experiments is performed inside a cabinet with a dimension of (82 cm, 50 cm, 37 cm) in the $X, Y,$

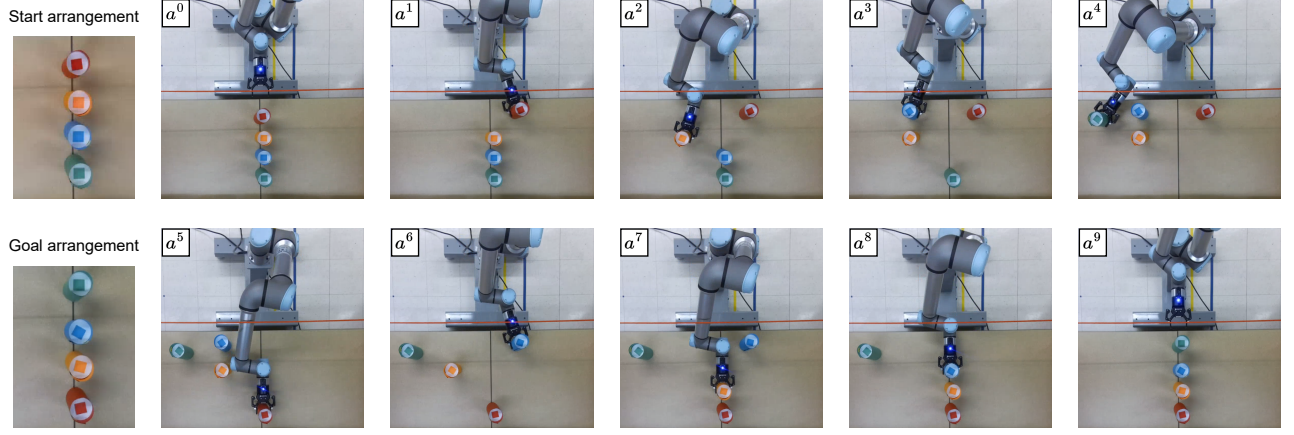


Fig. 3: This figure shows our MS-MCTS in action solving a four objects flipping case. The leftmost column presents the start arrangement and the desired goal arrangement. The images with labels on the top-left corner are the robot motion sequence taken from an overhead camera at the object relocation region.

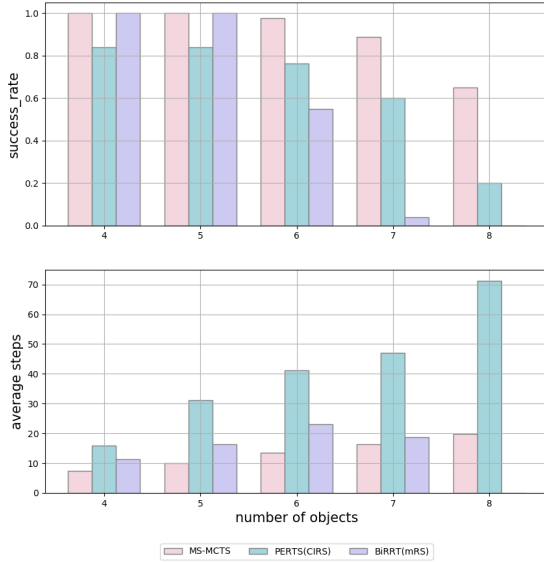


Fig. 4: Our MS-MCTS method has higher success rates but fewer steps than the baselines across all difficulty levels.

and Z axes, respectively. One of the testing cases that performs a four-object counter-clockwise rotation is shown in the left column of Figure 5. We can clearly see that the resulting plan follows the object stage topology and the goal arrangement is achieved without any unnecessary robot motion. To better observe the robot motion from a top-down view, the second confined environment with dimensions of (140 cm, 70 cm, 38 cm) is constructed on a table surrounded by cardboard blocks on the three sides as Figure 1 shows. The transparent “ceiling” is represented by a cable attached to the top of the opening. All robot parts should never touch or exceed the cable on the Z axis when it reaches inside the workspace during the rearrangement process. Otherwise, the experiment is considered a failure. Figure 3 shows a successfully performed four objects flipping case. We can easily observe that the planner only generates the necessary moves to fulfill the goal arrangement. Also, the objects are

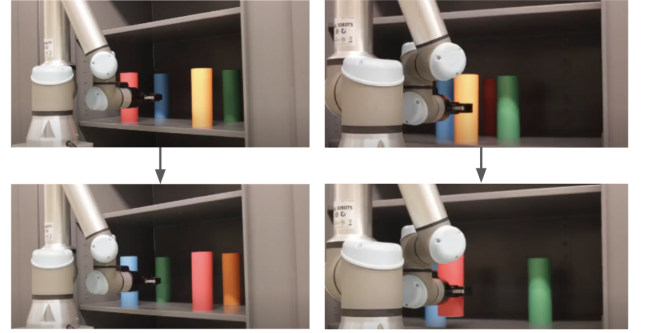


Fig. 5: The left column is the start arrangement and the achieved goal arrangement of a four objects counterclockwise rotation case while the right is an extension of our task planner applied to an object retrieval case.

relocated to the nearest buffer regions to minimize the sum of displacement distance.

2) *Object Retrieval*: Since object retrieval tasks can be viewed as a subset of object rearrangement tasks, our method can be naturally extended to solve them by running instances of SS-MCTS. The object to retrieve o_k should be set as the objective in the SS-MCTS. a^s is the current object arrangement, and a^g can be set exactly the same as a^s only with $a^g[o_k]$ changed to the beginning location of the gripper outside the environment. The reason behind these dummy settings is that the SS-MCTS focuses only on o_k and never makes excessive efforts to move other objects to their goal regions. The plan generated from the SS-MCTS retrieves the object o_k out of the confined narrow space. One of the examples is demonstrated in the right column of Figure 5. Compared with the existing arrangement planning algorithm that can also be used for object retrieval tasks, the SS-MCTS has two main advantages. First, the planner will never fail because of the invalid goal arrangements from imperfect sampling instances since we set the current arrangement as a dummy goal, which is always valid. Second, the planner only moves objects that truly prevent o_k from being

accessed, which better aligns with the idea of the object retrieval tasks.

VI. CONCLUSION

This paper presents our Multi-Stage MCTS algorithm that solves non-monotone object rearrangement planning tasks in narrow, confined spaces. Our method decouples the generally considered NP-hard problems into different ordered stages, with each stage focusing only on one object, which reduces the search space by a considerable amount. During relocation actions, the use of a linear motion planner minimizes the swept volume in the limited space and further leads to a higher chance of finding valid solutions. We fit the problem into the MCTS paradigm with customized designed functions to achieve high-quality results. The performance of our method is verified on various simulation cases with different difficulty levels and on the real robot.

For future works, we would like to add a robot active sensing module [30] so that the initial arrangements are observed by the robot efficiently instead of given as inputs. In addition, we also seek to extend the planner into the 3D space with objects of varying shapes and sizes. In such environments, different gripper orientations will be required for relocating objects due to force closure grasping constraints.

REFERENCES

- [1] J. Reif and M. Sharir, "Motion planning in the presence of moving obstacles," *Journal of the ACM (JACM)*, vol. 41, no. 4, pp. 764–790, 1994.
- [2] M. Stilman, K. Nishiwaki, S. Kagami, and J. J. Kuffner, "Planning and executing navigation among movable obstacles," *Advanced Robotics*, vol. 21, no. 14, pp. 1617–1634, 2007.
- [3] M. Stilman and J. Kuffner, "Planning among movable obstacles with artificial constraints," *The International Journal of Robotics Research*, vol. 27, no. 11-12, pp. 1295–1307, 2008.
- [4] M. Stilman, J.-U. Schamburek, J. Kuffner, and T. Asfour, "Manipulation planning among movable obstacles," in *Proceedings 2007 IEEE international conference on robotics and automation*. IEEE, 2007, pp. 3327–3332.
- [5] P. C. Chen and Y. K. Hwang, "Practical path planning among movable obstacles," Sandia National Labs., Albuquerque, NM (USA), Tech. Rep., 1990.
- [6] M. Stilman and J. J. Kuffner, "Navigation among movable obstacles: Real-time reasoning in complex environments," *International Journal of Humanoid Robotics*, vol. 2, no. 04, pp. 479–503, 2005.
- [7] C. R. Garrett, R. Chitnis, B. Holladay, B. Kim, T. Silver, L. P. Kaelbling, and T. Lozano-Pérez, "Integrated task and motion planning," *Annual review of control, robotics, and autonomous systems*, vol. 4, pp. 265–293, 2021.
- [8] S. Srivastava, E. Fang, L. Riano, R. Chitnis, S. Russell, and P. Abbeel, "Combined task and motion planning through an extensible planner-independent interface layer," in *2014 IEEE international conference on robotics and automation (ICRA)*. IEEE, 2014, pp. 639–646.
- [9] A. Krontiris and K. E. Bekris, "Efficiently solving general rearrangement tasks: A fast extension primitive for an incremental sampling-based planner," in *2016 IEEE International Conference on Robotics and Automation (ICRA)*. IEEE, 2016, pp. 3924–3931.
- [10] G. Havur, G. Ozbilgin, E. Erdem, and V. Patoglu, "Geometric rearrangement of multiple movable objects on cluttered surfaces: A hybrid reasoning approach," in *2014 IEEE International Conference on Robotics and Automation (ICRA)*. IEEE, 2014, pp. 445–452.
- [11] K. Gao, D. Lau, B. Huang, K. E. Bekris, and J. Yu, "Fast high-quality tabletop rearrangement in bounded workspace," in *2022 International Conference on Robotics and Automation (ICRA)*. IEEE, 2022, pp. 1961–1967.
- [12] W. Liu, C. Paxton, T. Hermans, and D. Fox, "Structformer: Learning spatial structure for language-guided semantic rearrangement of novel objects," in *2022 International Conference on Robotics and Automation (ICRA)*. IEEE, 2022, pp. 6322–6329.
- [13] A. H. Qureshi, A. Mousavian, C. Paxton, M. C. Yip, and D. Fox, "Nerp: Neural rearrangement planning for unknown objects," *arXiv preprint arXiv:2106.01352*, 2021.
- [14] A. Zeng, P. Florence, J. Tompson, S. Welker, J. Chien, M. Attarian, T. Armstrong, I. Krasin, D. Duong, V. Sindhwani *et al.*, "Transporter networks: Rearranging the visual world for robotic manipulation," in *Conference on Robot Learning*. PMLR, 2021, pp. 726–747.
- [15] W. Yuan, K. Hang, D. Kragic, M. Y. Wang, and J. A. Stork, "End-to-end nonprehensile rearrangement with deep reinforcement learning and simulation-to-reality transfer," *Robotics and Autonomous Systems*, vol. 119, pp. 119–134, 2019.
- [16] W. Yuan, J. A. Stork, D. Kragic, M. Y. Wang, and K. Hang, "Rearrangement with nonprehensile manipulation using deep reinforcement learning," in *2018 IEEE International Conference on Robotics and Automation (ICRA)*. IEEE, 2018, pp. 270–277.
- [17] R. Wang, Y. Miao, and K. E. Bekris, "Efficient and high-quality prehensile rearrangement in cluttered and confined spaces," in *2022 International Conference on Robotics and Automation (ICRA)*. IEEE, 2022, pp. 1968–1975.
- [18] R. Wang, K. Gao, D. Nakhimovich, J. Yu, and K. E. Bekris, "Uniform object rearrangement: From complete monotone primitives to efficient non-monotone informed search," in *2021 IEEE International Conference on Robotics and Automation (ICRA)*. IEEE, 2021, pp. 6621–6627.
- [19] R. Wang, K. Gao, J. Yu, and K. Bekris, "Lazy rearrangement planning in confined spaces," in *Proceedings of the International Conference on Automated Planning and Scheduling*, vol. 32, 2022, pp. 385–393.
- [20] J. Lee, C. Nam, J. Park, and C. Kim, "Tree search-based task and motion planning with prehensile and non-prehensile manipulation for obstacle rearrangement in clutter," in *2021 IEEE International Conference on Robotics and Automation (ICRA)*. IEEE, 2021, pp. 8516–8522.
- [21] C. B. Browne, E. Powley, D. Whitehouse, S. M. Lucas, P. I. Cowling, P. Rohlfshagen, S. Tavener, D. Perez, S. Samothrakis, and S. Colton, "A survey of monte carlo tree search methods," *IEEE Transactions on Computational Intelligence and AI in games*, vol. 4, no. 1, pp. 1–43, 2012.
- [22] D. Silver, T. Hubert, J. Schrittwieser, I. Antonoglou, M. Lai, A. Guez, M. Lanctot, L. Sifre, D. Kumaran, T. Graepel *et al.*, "A general reinforcement learning algorithm that masters chess, shogi, and go through self-play," *Science*, vol. 362, no. 6419, pp. 1140–1144, 2018.
- [23] M. C. Fu, "AlphaGo and monte carlo tree search: the simulation optimization perspective," in *2016 Winter Simulation Conference (WSC)*. IEEE, 2016, pp. 659–670.
- [24] T. M. Moerland, J. Broekens, A. Plaat, and C. M. Jonker, "A0c: Alpha zero in continuous action space," *arXiv preprint arXiv:1805.09613*, 2018.
- [25] Y. Labbé, S. Zagoruyko, I. Kalevtykh, I. Laptev, J. Carpentier, M. Aubry, and J. Sivic, "Monte-carlo tree search for efficient visually guided rearrangement planning," *IEEE Robotics and Automation Letters*, vol. 5, no. 2, pp. 3715–3722, 2020.
- [26] H. Song, J. A. Haustein, W. Yuan, K. Hang, M. Y. Wang, D. Kragic, and J. A. Stork, "Multi-object rearrangement with monte carlo tree search: A case study on planar nonprehensile sorting," in *2020 IEEE/RSJ International Conference on Intelligent Robots and Systems (IROS)*. IEEE, 2020, pp. 9433–9440.
- [27] J. E. King, V. Ranganeni, and S. S. Srinivasa, "Unobservable monte carlo planning for nonprehensile rearrangement tasks," in *2017 IEEE International Conference on Robotics and Automation (ICRA)*. IEEE, 2017, pp. 4681–4688.
- [28] S. K. Chan, "An iterative general inverse kinematics solution with variable damping," Ph.D. dissertation, University of British Columbia, 1987.
- [29] J. Huynh, "Separating axis theorem for oriented bounding boxes," URL: jk.me/files/tutorials/Separating%20Axis%20Theorem%20for%20Oriented%20Bounding%20Boxes.pdf, 2009.
- [30] H. Ren and A. H. Qureshi, "Robot active neural sensing and planning in unknown cluttered environments," *IEEE Transactions on Robotics*, pp. 1–13, 2023.